

Training Verification-Friendly Neural Networks via Neuron Behavior Consistency

Zongxin Liu^{1,2}, Zhe Zhao³, Fu Song^{1,4}, Jun Sun⁵, Pengfei Yang⁶, Xiaowei Huang⁷, Lijun Zhang^{1,2*}

¹Key Laboratory of System Software (Chinese Academy of Sciences) and State Key Laboratory of Computer Science,

Institute of Software, Chinese Academy of Sciences, Beijing, China

²University of Chinese Academy of Sciences, Beijing, China

³RealAI, Beijing, China

⁴Nanjing Institute of Software Technology, Nanjing, China

⁵Singapore Management University, Singapore

⁶College of Computer and Information Science, Software College, Southwest University, Chongqing, China

⁷The University of Liverpool, Liverpool, United Kingdom

liuzx@ios.ac.cn, zhe.zhao@realai.ai, songfu@ios.ac.cn, junsun@smu.edu.sg, ypfbest001@swu.edu.cn,

xiaowei.huang@liverpool.ac.uk, zhanglj@ios.ac.cn

Abstract

Formal verification provides critical security assurances for neural networks, yet its practical application suffers from the long verification time. This work introduces a novel method for training verification-friendly neural networks, which are robust, easy to verify, and relatively accurate. Our method integrates neuron behavior consistency into the training process, making neuron activation states consistent across different inputs in a local neighborhood, reducing the number of unstable neurons and tightening the bounds of neurons thereby enhancing neural network verifiability. We evaluated our method using the MNIST, Fashion-MNIST, and CIFAR-10 datasets across various network architectures. The results of the experiment demonstrate that networks trained using our method are verification-friendly across different radii and different model architectures, whereas other tools fail to maintain verifiability as the radius increases. We also show that our method can be combined with existing methods to further improve the verifiability of networks.

Introduction

Neural networks are increasingly applied in safety-critical domains such as autonomous driving (Urmson and Whitaker 2008) and flight control (Julian, Kochenderfer, and Owen 2019). However, they frequently struggle with a lack of robustness, as even minor perturbations to their inputs can lead to incorrect predictions (Bu et al. 2022; Chen et al. 2021; Song et al. 2021; Chen et al. 2023, 2022b; Zhao et al. 2021; Chen et al. 2022a). This is unacceptable in safety-critical applications, where consistent performance is imperative. Thus, it is desirable to develop methods to systematically advance the robustness verification of neural networks.

Existing methods for analyzing robustness can be divided into two categories: empirical analysis through adversarial attacks and mathematical proof via formal verification. While adversarial attacks generate misleading examples, they merely demonstrate the presence of adversarial

samples without affirming their absence. In contrast, formal verification ensures the correctness of neural networks using logical and mathematical methods, allowing us to formally verify the robustness of neural networks. This rigorous verification is essential for safety-critical systems.

Advanced formal verification tools (Wang et al. 2021; Zhang et al. 2022a; Bak 2021; Katz et al. 2017), typically employ branch-and-bound algorithms for neural network verification. At the beginning of verification, abstract interpretation (Gehr et al. 2018; Mirman, Gehr, and Vechev 2018; Zhang et al. 2021, 2023; Guo et al. 2021) is usually used to abstract neurons. If the properties of the network remain undetermined after using symbolic propagation (Singh et al. 2019) to calculate neuron boundaries and using MILP (Tjeng, Xiao, and Tedrake 2019; Tran et al. 2020; Zhang et al. 2022b; Zhang, Song, and Sun 2023; Zhang et al. 2024) or SMT methods (Ehlers 2017; Huang et al. 2017; Katz et al. 2017; Zhao et al. 2022; Liu et al. 2024) for constraint solving, further branching is required. The branching process involves enumerating the activation states of unstable neurons, whose activation status cannot be determined through bound calculations, to introduce additional constraints, thereby refining the abstraction. Typically, neural networks contain numerous unstable neurons, and exploring these combinations of activation states requires exponential time, which limits the widespread application of formal verification techniques in practice.

In addition to developing ever-more sophisticated methods for post-training verification, researchers have investigated the idea of training neural networks that are easier to verify, as known as verification-friendly neural networks. Ideally, a training method for verification-friendly neural networks must satisfy the following requirements. First, (accuracy) the resultant neural network must have an accuracy that is comparable to neural networks trained conventionally. Second, (robustness) the resultant neural network must have improved robustness, which could be measured using existing adversarial attacks. Third, (verifiability) it must be easier to verify using existing or dedicated neural network verification techniques, which can be measured using the ef-

*Corresponding author.

fectiveness of selected neural network verification methods.

There are mainly two existing approaches to promoting the verification-friendliness of neural networks. One approach involves post-processing the network through methods that modify the weights of the networks (Xiao et al. 2019; Baninajjar, Rezine, and Aminifar 2023). Another involves altering the neural network design and training process with considerations for verification (Xiao et al. 2019; Narodytska et al. 2019; Xu et al. 2024). However, these methods still have limitations. The effectiveness of post-training methods is limited by the network itself. Moreover, certain post-training methods such as using MILP to make the network more sparse (Baninajjar, Rezine, and Aminifar 2023), are computationally expensive and may not be adaptable for large networks. The ReLU Stable methods, which introduce ReLU Stable (RS) loss (Xiao et al. 2019) to reduce the number of unstable neurons, depend on the bounds of neurons, and when the perturbation radius changes, it often causes these bounds to shift, affecting the verification efficiency of the network. Certified training, mainly based on the heavy Interval Bound Propagation (IBP) method (Mirman, Gehr, and Vechev 2018; Gowal et al. 2018; Zhang et al. 2019a; Xu et al. 2020) suffers from a long training time and the gradient explosion or vanish problem. Adversarial training (Madry et al. 2018; Zhang et al. 2019b; Ganin et al. 2016; Zhu et al. 2017) typically increase network complexity but do not contribute to improving network verifiability.

In this work, we introduce a straightforward yet effective training method that enhances the verifiability of neural networks by enforcing the consistency of neuronal behavior, which we refer to as neuron behavior consistency (NBC), throughout the training process as a regularization term. A neuron is called behavior consistent if its activation state remains the same in a given input neighborhood. By maximizing the consistency of neurons, the unstable neurons are decreased, reducing the search space of the verification process. NBC can also help to tight the the bounds of neurons, as fewer unstable neurons introduce less error during bound calculation algorithms. Our approach can be scaled to larger networks compared to MILP-based methods. Moreover, the core of our method lies in the consistency of neuronal behavior without relying on heavy IBP methods, making a reduction in training epochs and ensuring the trained network maintains verifiability across different perturbation radii.

We evaluate our method using Fashion-MNIST, MNIST, and CIFAR-10 datasets across different architectures at various perturbation radii. Our method outperforms in stable neuron ratio and achieved up to a speedup of 450% in verification time. Importantly, our method accelerates the verification while preserving the accuracy of the model, which is not commonly achieved by existing methods. In summary, our contributions are as follows:

- We introduce a method of training verification-friendly networks by integrating neuron behavior consistency.
- We evaluated our methodology on three well-known datasets. Experiments show that networks trained using our method can maintain verification-friendly properties across different radii and different model architectures.

- We demonstrate that our method can be combined with existing methods to further improve the verifiability of networks, especially in the case of large networks.
- We show that our method accelerates the verification process while preserving model accuracy and robustness.

Preliminary

In this section, we introduce the background of neural network verification problems and the general branch and bound verification framework.

Neural Networks Verification Problems

Given a neural network $f : \mathbb{R}^{m_{\text{in}}} \rightarrow \mathbb{R}^{m_{\text{out}}}$, with m_{in} input neurons and m_{out} output neurons, the goal of the neural network verification problem is to determine whether the output of the network satisfies a set of output constraints \mathcal{P} for all inputs that meet the input constraints \mathcal{C} , formally defined as:

Definition 1 (Neural Network Verification Problem). *The neural network verification problem $\langle f, \mathcal{C}, \mathcal{P} \rangle$ is to determine whether:*

$$\forall \mathbf{x} \in \mathbb{R}^{m_{\text{in}}}, \mathbf{x} \in \mathcal{C} \Rightarrow f(\mathbf{x}) \in \mathcal{P}, \quad (1)$$

where $\mathcal{C} \subseteq \mathbb{R}^{m_{\text{in}}}$ is the input constraints and $\mathcal{P} \subseteq \mathbb{R}^{m_{\text{out}}}$ is the output constraints.

We focus on the local robustness verification problem $\langle f, \mathcal{C}_\epsilon(\mathbf{x}), \mathcal{P}_c \rangle$, which checks if the classification result c is robust to input perturbations ϵ in the norm l_∞ , where the input constraints $\mathcal{C}_\epsilon(\mathbf{x})$ defined as $\{\mathbf{x} \in \mathbb{R}^{m_{\text{in}}} \mid |\mathbf{x} - \mathbf{x}^0|_\infty \leq \epsilon\}$ and the output constraints \mathcal{P}_c defined as $\{\mathbf{y} \in \mathbb{R}^{m_{\text{out}}} \mid \bigwedge_{i \neq c} \mathbf{y}_i - \mathbf{y}_c \leq 0\}$.

General Verification Framework

State-of-the-art methods for solving neural network verification problems (Wang et al. 2021; Zhang et al. 2022a; Katz et al. 2019; Bak 2021) are typically based on branch-and-bound algorithms, consisting of three critical components: constraint solving, bound calculation, and branch selection.

As shown in Figure 1, the verification process starts with the bound calculation, where the upper and lower bounds of neuron output are estimated under specified input constraints. If these bounds are sufficiently precise, the properties of the network can be directly verified. Due to non-linear activation functions such as ReLU, computing these bounds can be complex, which is a problem often addressed through neuron-wise abstraction (Singh et al. 2019; Bak 2021). This abstraction uses linear bounds to approximate neuron outputs, thereby simplifying the bound calculations.

When the bound calculation does not suffice to verify the network’s properties, constraint solving is employed. This process involves determining if the constraints of the abstracted network can be satisfied, using Linear Programming (LP) or Mixed Integer Linear Programming (MILP) methods. Constraints typically include the input constraints \mathcal{C} , the negated output constraints $\neg \mathcal{P}$ and the constraints of the abstracted network itself. If these constraints are UNSAT (unsatisfiable), the property holds, which proves that the network can not be successfully attacked within \mathcal{C} ; otherwise, the returned counterexample must be examined. If

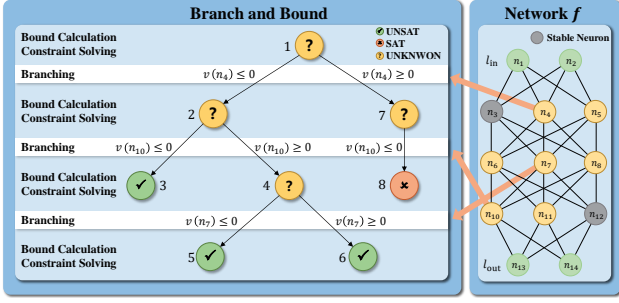


Figure 1: The Branch and Bound (BaB) verification process

the counterexample is not a false positive caused by over-approximation, a violation of the network’s properties is identified. Otherwise, it suggests that the network is over-abstracted, necessitating branch selection to refine the abstraction.

Branch selection selects an unstable neuron (whose activation state cannot be determined through bound calculations) and splits it into active and inactive branches. Identifying the state of a neuron entails establishing new constraints that refine the abstraction. Branch selection strategies critically affect verification efficiency. While branching may require exploration of all unstable neurons in worst-case scenarios, minimizing these neurons reduces the theoretical branching upper bound.

Training Verification-Friendly Networks via Neuron Behavior Consistency

In this section, we propose our method, neuron behavior consistency, to train verification-friendly neural networks.

Given a network f with parameters θ and an underlying distribution \mathcal{D} , the traditional training process aims to optimize the parameters θ to minimize the expected loss:

$$\min_{\theta} \mathbb{E}_{(\mathbf{x}, \mathbf{y}) \sim \mathcal{D}} (\text{loss}(\mathbf{x}, \mathbf{y})), \quad (2)$$

where (\mathbf{x}, \mathbf{y}) denotes the input and target label sampled from the distribution \mathcal{D} , and \mathbf{y} is the one-hot vector representation of the target label y , that is, a vector with a single 1 at the index of the target label and 0 elsewhere. The most common loss function is the cross-entropy function for classification tasks, defined as $\text{CE}(f(\mathbf{x}), \mathbf{y}) = -\sum_i \mathbf{y}_i \log f(\mathbf{x})_i$.

The ordinary training objective does not impose constraints on neurons, potentially resulting in a large number of unstable neurons. We thus propose an alternative training objective that aims to maximize the consistency of neurons. A neuron is consistent if its activation state remains the same in a given input neighborhood. Formally, given an input \mathbf{x} and a neighboring input \mathbf{x}' , the consistency of the j -th neuron of the i -th layer $n_j^{(i)}$ is defined as:

$$\text{NBC}(n_j^{(i)}, \mathbf{x}, \mathbf{x}') = \begin{cases} 1, & \text{if } \text{sign}(f^{(i)}(\mathbf{x})_j) = \text{sign}(f^{(i)}(\mathbf{x}')_j), \\ 0, & \text{otherwise,} \end{cases} \quad (3)$$

where $f^{(i)}(\mathbf{x})_j$ denotes the pre-activation value of the j -th neuron of the i -th layer when fed with input \mathbf{x} . Intuitively,

Algorithm 1: Calculation of NBC

Input: Neural network f , input \mathbf{x} , neighbor input \mathbf{x}'
Output: Neural behavior consistency between \mathbf{x} and \mathbf{x}'

```

1:  $s \leftarrow 0$ 
2: for the  $i$ -th layer  $l_i$  in hidden layers do
3:    $\mathbf{v} \leftarrow [f^{(i)}(\mathbf{x})_1, f^{(i)}(\mathbf{x})_2, \dots, f^{(i)}(\mathbf{x})_{m[i]}]^T$ 
4:    $\mathbf{v}' \leftarrow [f^{(i)}(\mathbf{x}')_1, f^{(i)}(\mathbf{x}')_2, \dots, f^{(i)}(\mathbf{x}')_{m[i]}]^T$ 
5:    $nbc \leftarrow \frac{\mathbf{v} \cdot \mathbf{v}'}{|\mathbf{v}| \cdot |\mathbf{v}'|}$ 
6:    $s \leftarrow s + \frac{nbc}{\gamma[i]}$ 
7: end for
8:  $s \leftarrow s - \text{KL}(f(\mathbf{x}) || f(\mathbf{x}'))$ 
9: return  $s$ 

```

for any input within a given neighborhood, if the activation states of individual neurons are highly consistent, the calculated boundaries (upper and lower bounds) are more likely to be tight. This coherence may reduce the occurrence of unstable neurons in the neural network.

To maximize (minimize the negative) this consistency, we incorporate a regularization term into the optimization objective, which can be represented as:

$$\min_{\theta} \mathbb{E}_{(\mathbf{x}, \mathbf{y}) \sim \mathcal{D}, \mathbf{x}' \in \mathcal{C}_{\varepsilon}(\mathbf{x})} [\text{CE}(f(\mathbf{x}), \mathbf{y}) - \beta \sum_{n_i \in \mathcal{N}} \text{NBC}(n_i, \mathbf{x}, \mathbf{x}')], \quad (4)$$

where β is a hyperparameter that controls the importance of the regularization term, and \mathcal{N} denotes the set of neurons in the network.

Adapting concepts from adversarial training, the loss function can be reformulated to maximize the minimal (minimize the negative minimal) consistency of neural behavior across different inputs within the neighborhood domain:

$$l^{\text{NBC}}(\mathbf{x}, \mathbf{y}) = \text{CE}(f(\mathbf{x}), \mathbf{y}) - \beta \min_{\mathbf{x}' \in \mathcal{C}_{\varepsilon}(\mathbf{x})} \sum_{n_i \in \mathcal{N}} \text{NBC}(n_i, \mathbf{x}, \mathbf{x}'). \quad (5)$$

The consistency metric presented in Equation 3 is a discrete measure that cannot be directly integrated into the loss function. Therefore, we employ a continuous metric to approximate the consistency of neural behavior across different inputs within the neighborhood domain, which is shown in Algorithm 1. This algorithm calculates the NBC between the neural network f when fed with \mathbf{x} and \mathbf{x}' .

During the calculation of NBC, the NBC value s is initially set to zero, then iterating over the hidden layers of f , the algorithm assesses the consistency for each neuron between the original and adversarial images, incrementally updating NBC. The final NBC is calculated as the sum of the scaled neuron consistencies across all layers.

Due to the characteristics of gradient backpropagation, the layer close to the output layer has a greater impact on the network’s behavior. Therefore, we use the KL divergence as a consistency metric for the output layer as a regularization term to ensure that the network’s output remains consistent across different inputs, which can be calculated as:

$$\text{KL}(f(\mathbf{x}) || f(\mathbf{x}')) = \sum_i f(\mathbf{x})_i \log \frac{f(\mathbf{x})_i}{f(\mathbf{x}')_i}. \quad (6)$$

For the hidden layers, to prevent gradient explosion or vanishing, we use cosine similarity as a continuous metric

Algorithm 2: Calculation of l^{NBC}

Input: Neural network f , input x , label y , perturbation ε , number of perturbation steps k , step size α , NBC regularization hyperparameter β

Output: Final NBC loss l^{NBC}

```
1: Generate a random starting point  $x' \in \mathcal{S}(x, \varepsilon)$ 
2: for  $i$  from 1 to  $k$  do
3:    $\Delta x \leftarrow \frac{\partial \text{NBC}(f, x, x')}{\partial x'}$ 
4:    $x' \leftarrow x' - \alpha \Delta x$ 
5:    $x' \leftarrow \text{clip}(x', x, \varepsilon)$ 
6: end for
7:  $l^{\text{NBC}} \leftarrow \text{CE}(f(x), y) - \beta \cdot \text{NBC}(f, x, x')$ 
8: return  $l^{\text{NBC}}$ 
```

to approximate the consistency of behavior, in which the output is in the range of $[0, 1]$, making it more suitable for training neural networks with high-dimensional intermediate layers. To balance the impact of layers with different numbers of neurons, we scale the NBC value by driving $\gamma[i]$ at line 6 of Algorithm 1. Our intuition is to prioritize layers with smaller dimensions as their consistent behavior may constrain subsequent layers through propagation. Moreover, input and output layers often have fewer neurons, applying constraints to them can directly affect the forward and backward propagation process and accelerate the convergence of target loss. In contrast, over-constraining middle layers, which have more neurons and extract complex features, could limit the model’s expressive power. Roughly speaking, using a looser penalty on layers with more neurons may slightly decrease accuracy but increase the proportion of stable neurons and improve verification speed. In our experiments, we apply factor $\gamma[i] = 2^{r[i]}$ to balance the impact of layers with different numbers of neurons, where $r[i]$ means the number of neurons in the i -th hidden layer is the $r[i]$ -th smallest number in all the numbers of neurons in hidden layers.

Algorithm 2 outlines the NBC loss calculation process. This algorithm uses the idea of adversarial training to find an adversarial input x' that minimizes the NBC loss between the input x and x' . The algorithm starts by randomly selecting an adversarial input x' within the ε -neighborhood of the original input x . Subsequently, the adversarial input undergoes iterative perturbation over k steps, with each perturbation step adjusting the adversarial input by gradients of the NBC for the adversarial input, scaled by the step size α . The adversarial input is clipped after each perturbation step to ensure that it remains within the perturbation range allowed from the original input. The final NBC loss is calculated as the summation of the cross-entropy loss and the negation of scaled NBC (Algorithm 1) between the original input and the adversarial input. Detailed discussion of the hyperparameters γ in Algorithm 1 and β in Algorithm 2 are provided in supplementary material.

We train the network to maximize neural response uniformity across varied inputs within the neighborhood, thereby reducing the number of unstable neurons and tightening neuronal bounds. Consequently, the network trained with NBC

loss is more friendly to formal verification methods, as it exhibits fewer unstable neurons and more precise bounds.

Evaluation

In this section, we evaluate our methods to answer the following research questions:

RQ1: Can networks trained with our method maintain their verification-friendly properties across various network architectures and radii?

RQ2: Can our method be effectively integrated with existing training methods?

RQ3: How does our method compare with existing methods under close accuracy ranges?

Experimental Setup

Experiments are conducted on a server with 128 Intel Xeon Platinum 8336C CPUs, 128GB memory, and four NVIDIA GeForce RTX 4090 GPUs, running Debian GNU/Linux 10 (Buster). We use Python 3.11.7 and PyTorch 2.1.2 for implementation. Other settings are as follows.

Dataset. Networks are trained on three widely used datasets, MNIST (LeCun et al. 1998), Fashion-MNIST (Xiao, Rasul, and Vollgraf 2017), and CIFAR-10 (Krizhevsky 2009).

Network Architecture. We select neural networks of varying sizes from VNN-COMP (Bak, Liu, and Johnson 2021; Müller et al. 2023) to assess the effectiveness of the methods used. For the MNIST and Fashion-MNIST datasets, we chose the M1 (cnn_4_layer), M2 (relu_stable), and M3 (conv_big) models, with approximately 0.16M, 0.17M, and 1.9M parameters, respectively. For the CIFAR-10 dataset, we select the C1 (marabou_medium), C2 (marabou_large), and C3 (conv_big) models, containing about 0.17M, 0.34M, and 2.4M parameters, respectively. Network architectures are detailed in supplementary material.

Baselines. We choose Relu Stable (Xiao et al. 2019) as a baseline, which shares the most similarities with our approach. TRADES (Zhang et al. 2019b) and Madry (Madry et al. 2018), two commonly used adversarial training methods, are selected to show that directly using our method can at least achieve robustness comparable to classical robust training methods and combining our method with existing methods can improve verification performance.

Training. We set the batch size to 128, the learning rate to 0.001, and employing the Adam optimizer. For RQ1, networks are trained under default settings for 400 epochs. For RQ2, each network underwent 200 epochs of training with the original method followed by another 200 epochs using a combination of the original and our methods, or in the reverse order. For RQ3, we use CE loss to train a base model and further fine-tune using RS, Madry, Trades, and our method separately to maintain each method’s accuracy within a specified range.

Verification. We use α, β -CROWN, a state-of-the-art verification tool that performs overall best in VNN-COMP competitions, to verify the properties of the trained networks. For each dataset, we select k images from each of the 10 categories in the test set. For each image x , and ground truth label y , we verified the property that the network’s output

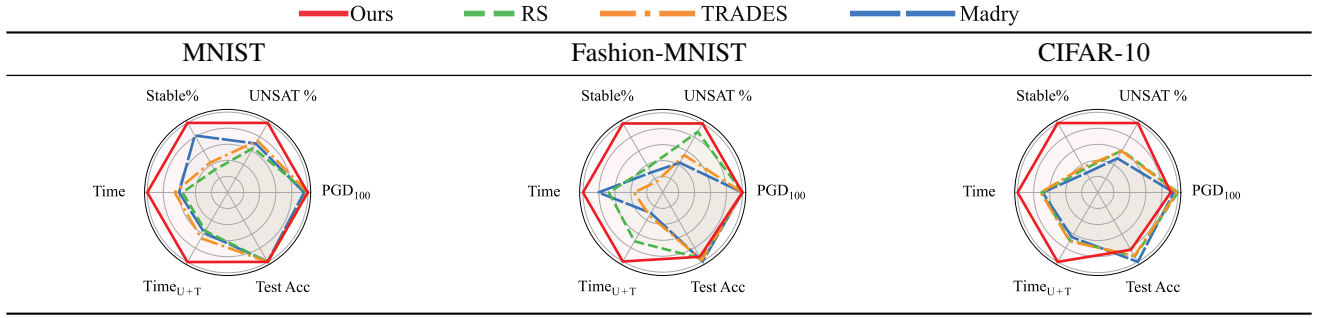


Figure 2: Overview of last epoch results. For each metric at each perturbation radius, the best-performing value is defined as 100, with other values scaled proportionally. We average all the scaled values of each model at each perturbation radius in each dataset to obtain the final score. For each metric, the larger value indicates better performance.

Model		M1				M2				M3			
Method		T	M	R	O	T	M	R	O	T	M	R	O
Test Acc.		99.0	98.2	98.9	98.8	99.1	98.3	99.2	98.9	99.1	99.3	99.3	99.0
$\varepsilon=0.1$	UNSAT%	96.6	95.0	96.4	97.2	96.8	93.0	96.9	97.0	94.5	87.8	86.0	96.6
	Stable%	72.0	84.7	68.0	84.7	69.4	81.5	65.9	86.6	78.4	69.3	48.4	92.1
	Time (s)	3.6	4.7	4.0	3.0	3.7	5.2	3.6	3.2	9.2	19.0	20.6	4.0
	Time _{U+T} (s)	3.5	4.5	3.9	2.9	3.6	5.0	3.5	3.1	8.9	19.1	20.7	3.9
	PGD ₁₀₀	97.6	95.9	97.7	97.7	97.8	94.3	97.9	97.9	98.0	97.6	98.2	97.9
$\varepsilon=0.2$	UNSAT%	89.5	86.7	79.0	92.2	85.6	71.3	71.8	91.8	2.3	0.2	1.5	46.3
	Stable%	34.8	65.7	25.2	64.5	27.7	66.1	20.5	68.0	17.2	10.0	4.3	68.7
	Time (s)	13.7	12.8	28.0	7.3	20.8	30.2	39.1	8.7	111.8	113.0	113.1	68.4
	Time _{U+T} (s)	14.1	13.1	29.7	7.3	21.6	33.8	41.2	8.8	117.5	119.8	118.3	71.9
	PGD ₁₀₀	95.7	91.8	95.0	95.6	96.0	88.8	95.8	96.4	96.1	95.5	96.0	96.0
$\varepsilon=0.3$	UNSAT%	29.4	35.5	7.0	60.1	13.3	8.2	3.9	47.4	0.0	0.0	0.0	0.0
	Stable%	6.2	40.7	2.4	47.8	2.9	37.2	1.4	53.9	0.1	0.0	0.0	52.5
	Time (s)	81.1	64.3	94.3	47.8	95.4	84.5	99.8	63.5	108.4	106.6	108.3	107.7
	Time _{U+T} (s)	91.5	80.0	113.8	55.0	108.5	113.0	116.6	72.9	120.0	120.0	120.0	120.0
	PGD ₁₀₀	93.1	83.3	89.3	91.3	92.8	80.0	91.8	91.4	92.2	91.3	91.6	91.9

Table 1: Networks trained with $\varepsilon = 0.3$ on MNIST datasets. The best results are highlighted in bold. Verified under $\varepsilon=0.1, 0.2, 0.3$. T:TRADES, M:Madry, R:ReLU Stable, O:Ours.

label remain y for input x under each perturbation ε . We set $k = 100$ and timeout at 120 seconds for MNIST and Fashion-MNIST, and $k = 20$ and timeout at 180 seconds for CIFAR-10.

Metrics. The metrics used in our evaluation are as follows:

- UNSAT%: The percentage of properties that are verified as holds (UNSAT), providing insight into the network’s overall verification effectiveness and verified robustness.
- Stable%: The average percentage of stable neurons, calculated as: $\frac{\sum_{i=1}^N s_i}{N}$, where s_i is stable neuron ratio of the i -th property, and N is the total number of properties.
- Time: The average time required to verify a property.
- Time_{U+T}: The average time is taken to verify properties resulting in UNSAT and Timeout. This metric is more indicative of the efficiency of the verification process, as it excludes the time taken to verify properties that are SAT, which can be verified quickly by attacking the network.
- PGD₁₀₀: The network’s accuracy under a PGD attack for 100 steps with a perturbation ε .

Results of the Last Epoch

Figure 2 shows the overall evaluation results of networks trained on MNIST, Fashion-MNIST, and CIFAR-10. As some metric values are too large or small, we set the best-performing value as 100 and other values are scaled proportionally to get a better visualization. Note that for metric Time and Time_{U+T}, we use the reciprocal of the values to make the visualization more intuitive. Therefore, the larger the metric in the table, the better the performance.

We observe that our method outperforms others in terms of verification time, stable neuron ratio, and verified ratio (UNSAT%). While our method slightly lags in accuracy and PGD accuracy, it generally maintains comparable accuracy to other methods. This result is a comprehensive evaluation across various perturbation radii and models, indicating that networks of various architectures trained using our method are more verification-friendly at different perturbation radii than those trained using other methods.

Table 1 shows the detailed results of networks trained on MNIST. Detailed results of Fashion-MNIST and CIFAR-10 are provided in the supplementary material. As shown in Ta-

Model		M1			M2			M3		
Method		T*	M*	R*	T*	M*	R*	T*	M*	R*
Test Acc.		-0.1	-3.9	-3.5	-0.1	-5.7	-2.8	-0.1	-0.4	-0.5
$\varepsilon=0.1$	UNSAT%	+0.6	-7.6	-4.3	-0.2	-11.2	-3.8	+2.0	+9.0	+10.6
	Stable%	+12.7	+12.8	+24.4	+16.4	+15.8	+25.6	+13.7	+25.3	+44.4
	Time (s)	-0.7	-1.1	-0.7	+1.1	+0.9	-0.3	-3.4	-14.8	-16.3
	Time _{U+T} (s)	-0.6	-1.4	-1.0	+1.1	+0.8	-0.5	-3.4	-15.1	-16.7
	PGD ₁₀₀	+0.1	-6.1	-4.3	-4.0	-7.9	-3.5	-0.2	+0.3	-0.4
$\varepsilon=0.2$	UNSAT%	+2.7	-10.0	+9.4	+4.9	-11.8	+18.0	+43.0	+83.2	+87.0
	Stable%	+29.7	+28.1	+57.9	+37.9	+26.2	+60.1	+51.0	+70.6	+74.6
	Time (s)	-6.4	-6.8	-23.9	-7.2	-12.3	-34.7	-41.9	-88.0	-97.3
	Time _{U+T} (s)	-6.8	-7.8	-26.0	-7.7	-11.5	-37.2	-44.4	-94.4	-102.5
	PGD ₁₀₀	-0.2	-9.9	-4.2	-2.2	-12.8	-4.1	-0.2	+0.4	-0.3
$\varepsilon=0.3$	UNSAT%	+30.7	+16.8	+72.4	+30.4	-0.6	+75.1	0.0	+4.4	+38.9
	Stable%	+41.6	+46.2	+69.1	+47.7	+39.5	+64.9	+51.7	+57.4	+53.8
	Time (s)	-33.3	-44.1	-86.2	-27.2	-32.6	-90.6	-0.5	-3.9	-40.8
	Time _{U+T} (s)	-36.5	-52.0	-105.9	-31.2	-6.4	-107.4	0.0	-4.4	-44.7
	PGD ₁₀₀	-1.5	-15.2	-3.0	+1.1	-21.6	-4.3	+0.2	+1.0	-0.4

Table 2: Networks trained with each method combined with our method on the MNIST dataset with $\varepsilon = 0.3$. Improved results are highlighted in bold. T*: TRADES+Ours, M*: Madry+Ours, R*: ReLU Stable+Ours.

ble 1, traditional adversarial training methods enhance network robustness, yet verifiability declines as the perturbation radius increases. This indicates the need for new training techniques that support effective verification. Regarding UNSAT%, our method consistently outperforms others, especially at higher perturbation radii. For instance, when $\varepsilon = 0.2$, our verified ratio reached 46.3%, which is more than 20 times that of the next best-performing method and over 231 times that of the least effective method on the M3 model. Unlike other methods, where UNSAT% significantly drops as the radius increases, our method maintains a high verified ratio across all tested radii.

As for stable neurons, our method excels across nearly all models and perturbation settings. Notably, in the M3 model at $\varepsilon = 0.3$, while competing methods exhibited virtually no stable neurons, our method preserved a stable neuron ratio above 50%. A higher proportion of stable neurons means if the verification time is increased, our method is more likely to be verified (as the search space is significantly reduced).

Regarding average verification time, including UNSAT and Timeout issues, our method generally requires less time across all verification tasks. An exception occurs in the M3 model at a 0.3 perturbation radius, where verification failed to confirm all the properties of our model. Conversely, the model trained using the Madry has many properties quickly verified as violated, thus shortening the times. Furthermore, under a 100-step PGD attack, our method achieved comparable accuracy to these adversarial training approaches. Such results also hold for Fashion-MNIST and CIFAR-10 datasets (see supplementary material).

Answer RQ1: Our method maintains high stable neuron ratios, UNSAT%, and robustness across various perturbation radii. Overall, networks trained with our method maintain their verification-friendly properties across various network architectures and radii.

Combination with Existing Methods

Table 2 shows the results of networks trained with our method combined with other methods on MNIST dataset. All examples show that our method combined with existing methods improves the ratio of stable neurons. In most cases, our method combined with existing methods increases the ratio of verified properties (UNSAT%) and reduces the time required for verification greatly.

It is worth noting that when the baseline method is combined with our method, the performance is particularly outstanding in larger network structures. For example, in the M3 model. Our method combined with Madry and RS methods respectively increased the verified ratio by 83.2% and 87.0% at $\varepsilon = 0.2$ and also decreased the time by 94.4 seconds and 102.5 seconds. This means that our method makes it possible to verify larger network structures. The same results are also reflected in the Fashion-MNIST and CIFAR-10 datasets provided in the supplementary material.

Combining our method with existing methods sacrifices some accuracy and adversarial accuracy, but improves verification and neural stability. In particular, the improvement is more pronounced in larger models. This means that our method makes it possible to verify larger network structures using existing verification tools. The same results are also reflected in the Fashion-MNIST and CIFAR datasets provided in the supplementary material.

Answer RQ2: Our method combined with other methods demonstrates to improve the verification-friendly properties of the network, however, a trade-off between accuracy and verifiability is required.

Comparison under Close Accuracy

The accuracy of networks trained using default parameters varied significantly on the CIFAR-10 dataset. To compare the performance of networks with close accuracy, we fine-

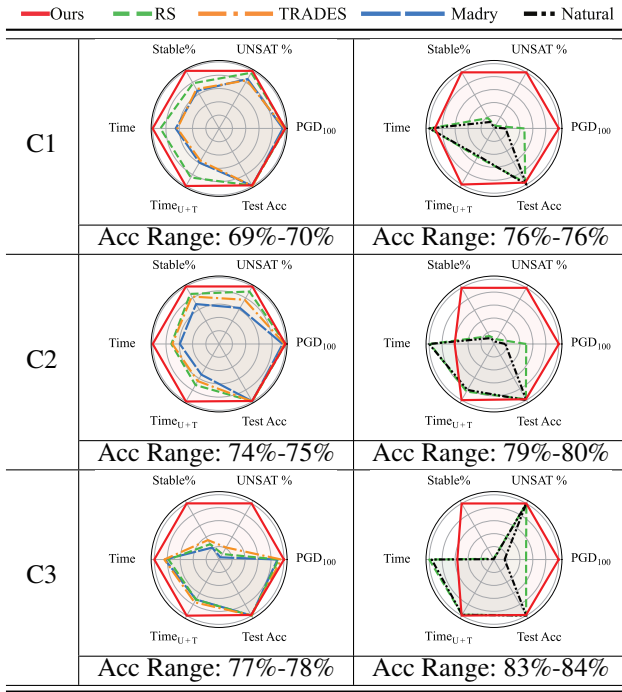


Figure 3: Networks trained with $\varepsilon = 2/255$ on CIFAR-10 dataset and evaluated on $\varepsilon = 2/255$. Methods unable to achieve given accuracy range are omitted. ‘Natural’ means the network are trained with only cross-entropy loss.

tuned the parameters to ensure that the accuracy of each method fluctuated within a certain range.

Figure 3 shows the results of networks trained on CIFAR-10. Larger perturbation radii are very challenging for current verification methods, so we choose a smaller perturbation radius to train and evaluate the networks.

In terms of UNSAT%, our method performs best in different network models and different accuracy ranges and generally requires less verification time for timeouts and UNSAT results than other methods, indicating that our networks are easier to verify. When the models reach higher accuracy, our method has a slightly longer average time, as other methods are more easily to find counterexamples using attack methods, while our method is less vulnerable to attacks.

Our accuracy under PGD is generally higher than other methods, with a few exceptions, where it is slightly lower than the best-performing method. Our method consistently maintains a higher ratio of stable neurons than other methods, especially in the C3 model, our method maintains a high ratio of stable neurons of up to 80.1% while maintaining a high verification accuracy, indicating that the upper bound of the search space is significantly reduced.

Answer RQ3: Experiments show that our method is more verification-friendly than other methods at higher and close accuracy levels, as our method consistently maintains a high ratio of stable neurons, and relative robustness and requires less verification time.

Related Work

Traditional adversarial methods such as TRADES (Zhang et al. 2019b) and Madry et al. (Madry et al. 2018) use adversarial training to improve the robustness of neural networks. However, these methods most impose constraints on the network output, while our method imposes neuron behavior constraints on all layers of the network. Recent works, HYDRA (Sehwag et al. 2020) integrates the pruning process with adversarial training, using a criterion that considers adversarial robustness during the pruning decision, leading to more compact yet robust models and Wu et al. (Wu, Xia, and Wang 2020) found that adversarial weight perturbation can improve the robustness of the network.

Certified training (De Palma et al. 2022; Mirman, Gehr, and Vechev 2018; Jovanovic et al. 2022; Zhang et al. 2019a; Xu et al. 2020) introduces interval bound propagation (IBP) into the training process to improve the robustness of the network but suffers from the long training time.

The ReLU Stable method (Xiao et al. 2019) ensures that the upper and lower bounds of the neurons have the same sign, pushing the upper and lower bounds away from zero in the same direction. This method can also incorporate ternary loss to train a SAT-friendly network (Narodytska et al. 2019). In contrast, our method emphasizes the stability of neurons before and after perturbation, focusing on the similarity and consistency of neuron behavior. Furthermore, RS loss requires additional calculations for each neuron’s bounds, whereas our method does not require extra information, making it easier to implement. Linearity grafting (Chen et al. 2022c) replaces unstable neurons with linear neurons to improve the robustness of the network. However, this method will modify network architectures, while our method keeps the architecture unchanged. MILP-based method (Baninajjar, Rezine, and Aminifar 2023) uses MILP to post-process the network to make it sparse to improve the verification efficiency, which may be time-consuming. Pruning-based methods (Xiao et al. 2019; Xu et al. 2024) heuristically prune the neurons that are inactive or unstable and have little impact on the network’s performance. Bias shaping method (Xu et al. 2024) changing the bias of the unstable neurons during training to stabilize them. These methods are either post-processing methods or training tricks that can be incorporated with other methods to further improve the verifiability of networks.

Conclusion

In this work, we propose a novel training method to train a verification-friendly neural network by preserving the neuron behavior consistency of the network. Our experiments on the MNIST, Fashion-MNIST, and CIFAR-10 datasets demonstrate that our method consistently enhances the network’s verification-friendliness, as evidenced by a stable neuron ratio, comparable robustness, and faster verification speed across different perturbation radii. Additionally, existing methods, when combined with ours, show improved verification efficiency. Our method also speeds up the verification process while maintaining the accuracy of the model, which is not commonly achieved by existing methods.

Acknowledgements

This work is partly supported by CAS Project for Young Scientists in Basic Research, Grant No.YSBR-040, ISCAS New Cultivation Project ISCAS-PYFX-202201, ISCAS Basic Research ISCAS-JCZD-202302 and the Ministry of Education, Singapore under its Academic Research Fund Tier 3 (Award ID: MOET32020-0004).

References

- Bak, S. 2021. nnenum: Verification of ReLU neural networks with optimized abstraction refinement. In *Proceedings of the 13th International Symposium on NASA Formal Methods (NFM)*, 19–36. Springer.
- Bak, S.; Liu, C.; and Johnson, T. T. 2021. The Second International Verification of Neural Networks Competition (VNN-COMP 2021): Summary and Results. *CoRR*, abs/2109.00498.
- Baninajjar, A.; Rezine, A.; and Aminifar, A. 2023. Verification-Friendly Deep Neural Networks. *arXiv preprint arXiv:2312.09748*.
- Bu, L.; Zhao, Z.; Duan, Y.; and Song, F. 2022. Taking Care of the Discretization Problem: A Comprehensive Study of the Discretization Problem and a Black-Box Adversarial Attack in Discrete Integer Domain. *IEEE Trans. Dependable Secur. Comput.*, 19(5): 3200–3217.
- Chen, G.; Chen, S.; Fan, L.; Du, X.; Zhao, Z.; Song, F.; and Liu, Y. 2021. Who is Real Bob? Adversarial Attacks on Speaker Recognition Systems. In *Proceedings of the 42nd IEEE Symposium on Security and Privacy (S&P)*, 694–711.
- Chen, G.; Zhang, Y.; Zhao, Z.; and Song, F. 2023. QFA2SR: Query-Free Adversarial Transfer Attacks to Speaker Recognition Systems. In *Proceedings of the 32nd USENIX Security Symposium*.
- Chen, G.; Zhao, Z.; Song, F.; Chen, S.; Fan, L.; ; Wang, F.; and Wang, J. 2022a. Towards Understanding and Mitigating Audio Adversarial Examples for Speaker Recognition. *IEEE Trans. Dependable Secur. Comput.*, 1–17.
- Chen, G.; Zhao, Z.; Song, F.; Chen, S.; Fan, L.; and Liu, Y. 2022b. AS2T: Arbitrary Source-To-Target Adversarial Attack on Speaker Recognition Systems. *IEEE Trans. Dependable Secur. Comput.*, 1–17.
- Chen, T.; Zhang, H.; Zhang, Z.; Chang, S.; Liu, S.; Chen, P.-Y.; and Wang, Z. 2022c. Linearity grafting: Relaxed neuron pruning helps certifiable robustness. In *Proceedings of the International Conference on Machine Learning (ICML)*, 3760–3772. PMLR.
- De Palma, A.; Bunel, R.; Dvijotham, K.; Kumar, M. P.; and Stanforth, R. 2022. IBP regularization for verified adversarial robustness via branch-and-bound. *arXiv preprint arXiv:2206.14772*.
- Ehlers, R. 2017. Formal verification of piece-wise linear feed-forward neural networks. In *Proceedings of the 15th International Symposium on Automated Technology for Verification and Analysis (ATVA)*, 269–286. Springer.
- Ganin, Y.; Ustinova, E.; Ajakan, H.; Germain, P.; Larochelle, H.; Laviolette, F.; Marchand, M.; and Lempitsky, V. 2016. Domain-adversarial training of neural networks. *The journal of machine learning research*, 17(1): 2096–2030.
- Gehr, T.; Mirman, M.; Drachler-Cohen, D.; Tsankov, P.; Chaudhuri, S.; and Vechev, M. 2018. Ai2: Safety and robustness certification of neural networks with abstract interpretation. In *Proceedings of the IEEE symposium on security and privacy (SP)*, 3–18. IEEE.
- Gowal, S.; Dvijotham, K.; Stanforth, R.; Bunel, R.; Qin, C.; Uesato, J.; Arandjelovic, R.; Mann, T. A.; and Kohli, P. 2018. On the Effectiveness of Interval Bound Propagation for Training Verifiably Robust Models. *CoRR*, abs/1810.12715.
- Guo, X.; Wan, W.; Zhang, Z.; Zhang, M.; Song, F.; and Wen, X. 2021. Eager Falsification for Accelerating Robustness Verification of Deep Neural Networks. In Jin, Z.; Li, X.; Xiang, J.; Mariani, L.; Liu, T.; Yu, X.; and Ivaki, N., eds., *Proceedings of the 32nd IEEE International Symposium on Software Reliability Engineering (ISSRE)*, 345–356. IEEE.
- Huang, X.; Kwiatkowska, M.; Wang, S.; and Wu, M. 2017. Safety verification of deep neural networks. In *Proceedings of the 29th International Conference on Computer Aided Verification (CAV)*, 3–29. Springer.
- Jovanovic, N.; Balunovic, M.; Baader, M.; and Vechev, M. T. 2022. On the Paradox of Certified Training. *Trans. Mach. Learn. Res.*
- Julian, K. D.; Kochenderfer, M. J.; and Owen, M. P. 2019. Deep neural network compression for aircraft collision avoidance systems. *Journal of Guidance, Control, and Dynamics*, 42(3): 598–608.
- Katz, G.; Barrett, C.; Dill, D. L.; Julian, K.; and Kochenderfer, M. J. 2017. Reluplex: An efficient SMT solver for verifying deep neural networks. In *Proceedings of the 29th International Conference on Computer Aided Verification (CAV)*, 97–117. Springer.
- Katz, G.; Huang, D. A.; Ibeling, D.; Julian, K.; Lazarus, C.; Lim, R.; Shah, P.; Thakoor, S.; Wu, H.; Zeljic, A.; Dill, D. L.; Kochenderfer, M. J.; and Barrett, C. W. 2019. The Marabou Framework for Verification and Analysis of Deep Neural Networks. In *Proceedings of the 31th International Conference on Computer Aided Verification (CAV)*, 443–452.
- Krizhevsky, A. 2009. Learning Multiple Layers of Features from Tiny Images.
- LeCun, Y.; Bottou, L.; Bengio, Y.; and Haffner, P. 1998. Gradient-based learning applied to document recognition. *Proc. IEEE*, 86(11): 2278–2324.
- Liu, J.; Xing, Y.; Shi, X.; Song, F.; Xu, Z.; and Ming, Z. 2024. Abstraction and Refinement: Towards Scalable and Exact Verification of Neural Networks. *ACM Trans. Softw. Eng. Methodol.*, 33(5): 129:1–129:35.
- Madry, A.; Makelov, A.; Schmidt, L.; Tsipras, D.; and Vladu, A. 2018. Towards Deep Learning Models Resistant to Adversarial Attacks. In *Proceedings of the 6th International Conference on Learning Representations (ICLR)*.
- Mirman, M.; Gehr, T.; and Vechev, M. 2018. Differentiable abstract interpretation for provably robust neural networks. In *Proceedings of the International Conference on Machine Learning (ICML)*, 3578–3586. PMLR.

- Müller, M. N.; Brix, C.; Bak, S.; Liu, C.; and Johnson, T. T. 2023. The Third International Verification of Neural Networks Competition (VNN-COMP 2022): Summary and Results. *arXiv:2212.10376*.
- Narodytska, N.; Zhang, H.; Gupta, A.; and Walsh, T. 2019. In search for a SAT-friendly binarized neural network architecture. In *Proceedings of the International Conference on Learning Representations (ICLR)*.
- Sehwag, V.; Wang, S.; Mittal, P.; and Jana, S. 2020. Hydra: Pruning adversarially robust neural networks. *Advances in Neural Information Processing Systems*, 33: 19655–19666.
- Singh, G.; Gehr, T.; Püschel, M.; and Vechev, M. T. 2019. An abstract domain for certifying neural networks. *PACMPL*, 3(POPL): 41:1–41:30.
- Song, F.; Lei, Y.; Chen, S.; Fan, L.; and Liu, Y. 2021. Advanced evasion attacks and mitigations on practical ML-based phishing website classifiers. *Int. J. Intell. Syst.*, 36(9): 5210–5240.
- Tjeng, V.; Xiao, K. Y.; and Tedrake, R. 2019. Evaluating Robustness of Neural Networks with Mixed Integer Programming. In *7th International Conference on Learning Representations (ICLR)*.
- Tran, H.-D.; Yang, X.; Manzananas Lopez, D.; Musau, P.; Nguyen, L. V.; Xiang, W.; Bak, S.; and Johnson, T. T. 2020. NNV: the neural network verification tool for deep neural networks and learning-enabled cyber-physical systems. In *International Conference on Computer Aided Verification*, 3–17. Springer.
- Urmson, C.; and Whittaker, W. 2008. Self-Driving Cars and the Urban Challenge. *IEEE Intell. Syst.*, 23(2): 66–68.
- Wang, S.; Zhang, H.; Xu, K.; Lin, X.; Jana, S.; Hsieh, C.-J.; and Kolter, J. Z. 2021. Beta-CROWN: Efficient bound propagation with per-neuron split constraints for neural network robustness verification. *Advances in Neural Information Processing Systems*, 34: 29909–29921.
- Wu, D.; Xia, S.-T.; and Wang, Y. 2020. Adversarial weight perturbation helps robust generalization. *Advances in neural information processing systems*, 33: 2958–2969.
- Xiao, H.; Rasul, K.; and Vollgraf, R. 2017. Fashion-MNIST: a Novel Image Dataset for Benchmarking Machine Learning Algorithms. *CoRR*, abs/1708.07747.
- Xiao, K. Y.; Tjeng, V.; Shafiullah, N. M. M.; and Madry, A. 2019. Training for Faster Adversarial Robustness Verification via Inducing ReLU Stability. In *7th International Conference on Learning Representations (ICLR)*.
- Xu, D.; Mozumder, N. J.; Duong, H.; and Dwyer, M. B. 2024. Training for Verification: Increasing Neuron Stability to Scale DNN Verification. In Finkbeiner, B.; and Kovács, L., eds., *Proceedings of the 30th International Conference on Tools and Algorithms for the Construction and Analysis of Systems (TACAS)*, 24–44. Springer.
- Xu, K.; Shi, Z.; Zhang, H.; Wang, Y.; Chang, K.-W.; Huang, M.; Kailkhura, B.; Lin, X.; and Hsieh, C.-J. 2020. Automatic perturbation analysis for scalable certified robustness and beyond. *Advances in Neural Information Processing Systems*, 33: 1129–1141.
- Zhang, H.; Chen, H.; Xiao, C.; Goyal, S.; Stanforth, R.; Li, B.; Boning, D.; and Hsieh, C.-J. 2019a. Towards stable and efficient training of verifiably robust neural networks. *arXiv preprint arXiv:1906.06316*.
- Zhang, H.; Wang, S.; Xu, K.; Li, L.; Li, B.; Jana, S.; Hsieh, C.; and Kolter, J. Z. 2022a. General Cutting Planes for Bound-Propagation-Based Neural Network Verification. In *NeurIPS*.
- Zhang, H.; Yu, Y.; Jiao, J.; Xing, E. P.; Ghaoui, L. E.; and Jordan, M. I. 2019b. Theoretically Principled Trade-off between Robustness and Accuracy. In *Proceedings of the 36th International Conference on Machine Learning (ICML)*, volume 97, 7472–7482. PMLR.
- Zhang, Y.; Chen, G.; Song, F.; Sun, J.; and Dong, J. S. 2024. Certified Quantization Strategy Synthesis for Neural Networks. In Platzer, A.; Rozier, K. Y.; Pradella, M.; and Rossi, M., eds., *Proceedings of the 26th International Symposium on Formal Methods (FM)*, 343–362. Springer.
- Zhang, Y.; Song, F.; and Sun, J. 2023. QEBVerif: Quantization Error Bound Verification of Neural Networks. In Enea, C.; and Lal, A., eds., *Proceedings of the 35th International Conference on Computer Aided Verification (CAV)*, volume 13965, 413–437. Springer.
- Zhang, Y.; Zhao, Z.; Chen, G.; Song, F.; and Chen, T. 2021. BDD4BNN: A BDD-Based Quantitative Analysis Framework for Binarized Neural Networks. In Silva, A.; and Leino, K. R. M., eds., *Proceedings of the 33rd International Conference on Computer Aided Verification*, 175–200.
- Zhang, Y.; Zhao, Z.; Chen, G.; Song, F.; and Chen, T. 2023. Precise Quantitative Analysis of Binarized Neural Networks: A BDD-based Approach. *ACM Trans. Softw. Eng. Methodol.*, 32(3): 62:1–62:51.
- Zhang, Y.; Zhao, Z.; Chen, G.; Song, F.; Zhang, M.; Chen, T.; and Sun, J. 2022b. QVIP: An ILP-based Formal Verification Approach for Quantized Neural Networks. In *Proceedings of the 37th IEEE/ACM International Conference on Automated Software Engineering (ASE)*, 82:1–82:13. ACM.
- Zhao, Z.; Chen, G.; Wang, J.; Yang, Y.; Song, F.; and Sun, J. 2021. Attack as defense: characterizing adversarial examples using robustness. In *Proceedings of the 30th ACM SIGSOFT International Symposium on Software Testing and Analysis (ISSTA)*, 42–55.
- Zhao, Z.; Zhang, Y.; Chen, G.; Song, F.; Chen, T.; and Liu, J. 2022. CLEVEREST: Accelerating CEGAR-based Neural Network Verification via Adversarial Attacks. In Singh, G.; and Urban, C., eds., *Proceedings of the 29th International Symposium on Static Analysis (SAS)*, 449–473. Springer.
- Zhu, J.-Y.; Park, T.; Isola, P.; and Efros, A. A. 2017. Unpaired Image-to-Image Translation Using Cycle-Consistent Adversarial Networks. In *Proceedings of the IEEE International Conference on Computer Vision (ICCV)*, 2242–2251.

Detailed Experimental Setup

Dataset Selection.

We select three datasets: Fashion-MNIST, MNIST, and CIFAR-10 datasets for our experiments. The MNIST and CIFAR-10 datasets are widely used in early adversarial training research (Madry et al. 2018; Zhang et al. 2019b) and similar studies (Xiao et al. 2019; Xu et al. 2024). To demonstrate the generality of our method, we additionally included the Fashion-MNIST dataset. The categories in the Fashion-MNIST dataset are similar to those in the MNIST dataset, but the images in the Fashion-MNIST dataset are more complex and challenging compared to the MNIST dataset.

Network Architecture Selection.

We select the following network architectures based on the network sizes used in previous works (Xiao et al. 2019; Xu et al. 2024), the verification capabilities of neural network verification tools, and the generality of the networks. M1 and C1 are smaller networks, M2 and C2 are medium-sized networks, and M3 and C3 are larger networks. Compared to previous works, we mostly use convolutional networks instead of fully connected networks. This is because the use of convolutional networks is more common in real applications. Moreover, M3 and C3 are even larger than the largest network structures used in similar works (Xiao et al. 2019; Xu et al. 2024) and are very close to the limits of neural network verification tools. Table 3 provides detailed descriptions of the network architectures used in our experiments.

Training Details.

For the MNIST and the Fashion-MNIST datasets, we directly use the original pictures to train each network. For the CIFAR-10 dataset, we randomly crop images to 32x32 pixels and augment the data by flipping images horizontally with a probability of 0.5. We also add padding of 4 pixels on each side before cropping.

We use the Adam optimizer to train all networks with a batch size of 128. The learning rate is set to 0.0001 for the MNIST and Fashion-MNIST datasets and 0.00001 for the CIFAR-10 dataset. We use the same number of training iterations for all datasets, which is 400 iterations. The random seed is set to 0 for reproducibility. All PGD-like adversarial training process uses the same hyperparameters as 10 steps and a step size of $\varepsilon/10$.

In the last epoch experiment, for the RS (Xiao et al. 2019), Madry (Madry et al. 2018), and TRADES (Zhang et al. 2019b) methods, we used the same hyperparameters as in the original papers. As for our model, we use the hyperparameters $\beta = 1$ for M1, M2 and M3 models, and $\beta = 2, 5, 3$ for C1, C2, and C3 models, respectively. We select the hyperparameters based on the performance of the model on the validation set (generated by the original training set).

In the combination experiment, we find that different methods have different performances when using different combination orders. Based on the performance of the model on the validation set. For the RS method, we first train 200 epochs using the original RS loss and then combine it with our NBC loss for another 200 epochs. For the Madry method, we use the method combined with NBC loss for 200 epochs and then use the original Madry loss for another

200 epochs. For the TRADES method, we use the method combined with the NBC loss to train directly for 400 epochs. The parameters are the same as the original training process.

The application of these methods results mainly in a decrease in accuracy compared to direct training without these methods, which may be unacceptable in practical applications. Therefore, our objective is to evaluate the effectiveness of these methods while maintaining relatively high accuracy. We specified two sets of accuracy ranges for each model: one where the accuracy difference from the 'Natural' method is within 1%-2%, and another where the difference is within 6%-7%. We believe this setup effectively evaluates the effectiveness of each method under different accuracy requirements. Besides, as shown in Table 1 and 5, various metrics drop as the robustness radius increases, making the differences in metrics between various methods less apparent. The use of $\varepsilon = 2/255$ to train the model and the same ε to verify the model reveals the differences more clearly and better illustrates the issue. In this experiment, we initially trained a baseline network using only cross-entropy loss (referred to as 'Natural' in the tables and figures). We then used this model as a pre-trained baseline and applied various methods to fine-tune it separately, aiming to achieve a relatively high accuracy.

Verification Tasks.

To demonstrate that our methods have generalization capabilities, we train on the training set and generate local robustness verification tasks under different perturbation radii on the test set. We use the same verification tasks for all methods to ensure fairness.

Detailed Experimental Results

The following tables provide detailed results of the experiments conducted for RQ1, RQ2, and RQ3. Typically, Table 4, 5 and Table 6, 7 show the results of networks trained for RQ1 and RQ2, on Fashion-MNIST and CIFAR-10 datasets, respectively. Table 8 shows the results of networks trained for RQ3 on CIFAR-10 datasets.

Extra Results for RQ1

Table 4 shows the evaluation results of networks trained in Fashion-MNIST.

In the M1 model, our method demonstrates moderate accuracy. Although our method is not the best in terms of UNSAT%, it is within 1% of the best performing RS method. Our method performs best in terms of UNSAT% at $\varepsilon = 0.3$. Our method consistently maintains the best performance in terms of stability, with a stable ratio of over 50%. Our method is the fastest in terms of verification time, and its advantage becomes more pronounced as the perturbation radius increases. Our method performs moderately under the PGD attack.

In the M2 model, our method still performs best in terms of Stable%. However, various methods have their advantages and disadvantages.

It should be noted that in the M3 model, our method performs best in terms of UNSAT%, Stable%, and the average time of UNSAT and timeout issues. Especially at $\varepsilon = 0.3$,

Dataset	Architecture Name	#Parameters	Network Architecture
(Fashion-) MNIST	Cnn 4layer (M1)	166,406	Conv2d(1, 16, (4, 4), (2, 2), (1, 1)) Conv2d(16, 32, (4, 4), (2, 2), (1, 1)) Linear(1568, 100), Linear(100, 10)
	Relu Stable (M2)	171,158	Conv2d(1, 16, (5, 5), (2, 2), (2, 2)) Conv2d(16, 32, (5, 5), (2, 2), (2, 2)) Linear(1568, 100), Linear(100, 10)
	Conv Big (M3)	1,974,762	Conv2d(1, 32, (3, 3), (1, 1), (1, 1)) Conv2d(32, 32, (4, 4), (2, 2), (1, 1)) Conv2d(32, 64, (3, 3), (1, 1), (1, 1)) Conv2d(64, 64, (3, 3), (2, 2), (1, 1)) Linear(3316, 512), Linear(512, 512) Linear(512, 10)
CIFAR-10	Marabou medium (C1)	165,498	Conv2d(3, 16, (4, 4), (2, 2), (2, 2)) Conv2d(16, 32, (4, 4), (2, 2), (2, 2)) Linear(1152, 128), Linear(128, 64) Linear(64, 10)
	Marabou large (C2)	338,346	Conv2d(3, 16, (4, 4), (2, 2), (2, 2)) Conv2d(16, 32, (4, 4), (2, 2), (2, 2)) Linear(2304, 128), Linear(128, 64) Linear(64, 10)
	Conv Big (C3)	2,466,858	Conv2d(3, 32, (3, 3), (1, 1), (1, 1)) Conv2d(32, 32, (4, 4), (2, 2), (1, 1)) Conv2d(32, 64, (3, 3), (1, 1), (1, 1)) Conv2d(64, 64, (3, 3), (2, 2), (1, 1)) Linear(4096, 512), Linear(512, 512) Linear(512, 10)

Table 3: Network Architectures for Experiments

Model		M1				M2				M3			
Method		T	M	R	O	T	M	R	O	T	M	R	O
Test Acc.		84.0	84.4	81.3	82.1	83.8	86.0	80.5	78.3	87.2	89.3	86.2	81.6
$\varepsilon=0.1$	UNSAT%	53.5	30.6	70.1	69.1	49.3	2.0	70.0	65.5	16.3	0.2	27.1	63.3
	Stable%	36.6	66.7	68.0	78.9	31.1	47.7	65.2	86.2	4.4	3.8	6.7	84.4
	Time (s)	25.2	26.5	9.5	6.8	29.7	19.3	9.4	8.0	79.7	33.0	68.4	20.4
	Time _{U+T} (s)	32.7	46.5	9.2	6.3	40.5	103.5	9.9	7.9	97.8	118.6	82.7	22.1
	PGD ₁₀₀	70.5	49.5	73.8	71.8	68.9	30.5	73.6	71.1	77.5	31.8	78.1	74.7
$\varepsilon=0.2$	UNSAT%	24.8	6.0	55.4	54.5	9.9	0.1	54.2	46.0	0.0	0.0	0.8	42.4
	Stable%	15.1	34.0	37.7	63.3	9.8	17.3	34.9	70.1	0.0	0.2	0.1	63.2
	Time (s)	48.6	42.7	15.7	9.5	61.2	13.8	16.9	22.0	82.0	32.1	83.6	36.9
	Time _{U+T} (s)	78.1	104.5	18.8	10.4	105.4	119.7	22.1	32.0	120.0	120.0	118.9	48.7
	PGD ₁₀₀	62.7	42.5	66.3	61.8	62.6	32.5	67.1	65.0	68.8	31.2	70.8	67.9
$\varepsilon=0.3$	UNSAT%	5.3	0.4	31.2	35.6	0.2	0.0	30.0	17.4	0.0	0.0	0.0	17.4
	Stable%	6.2	15.2	14.4	54.2	1.9	5.8	12.6	57.4	0.0	0.0	0.0	43.8
	Time (s)	52.6	34.6	30.6	16.4	49.5	10.4	33.2	41.2	62.8	34.6	69.2	51.0
	Time _{U+T} (s)	109.9	118.5	50.7	27.0	119.6	120.0	56.8	79.8	120.0	120.0	120.0	85.4
	PGD ₁₀₀	53.1	36.7	57.3	49.4	51.1	31.7	58.9	59.5	58.3	36.8	62.2	59.5

Table 4: Networks trained with $\varepsilon = 0.3$ on Fashion-MNIST datasets. The best results are highlighted in bold. Verified under $\varepsilon=0.1, 0.2, 0.3$. T:TRADES, M:Madry, R:ReLU Stable, O:Ours.

our method performs best in terms of UNSAT%, reaching 17.4%, while networks trained with other methods cannot verify any UNSAT properties. Our method performs moderately under the PGD attack.

Table 5 shows the evaluation results of networks trained on CIFAR-10. Although our method does not perform well on test set accuracy compared to other approaches, it outperforms other metrics.

Our method demonstrates superior performance in terms

of the average verification speed and the average speed of UNSAT and Timeout issues, requiring less verification time on almost all verification tasks. This is especially evident in the C1 and C2 models, where our method consistently outperforms other approaches in terms of verification time. Although the accuracy under 100 steps of the PGD attack is not the best-performing method, our method still achieves competitive PGD accuracy.

Our method outperforms others in terms of verification

Model		C1				C2				C3			
Method		T	M	R	O	T	M	R	O	T	M	R	O
Test Acc.		59.2	62.8	56.0	51.8	60.9	69.5	61.8	54.9	69.5	75.5	74.1	64.9
$\frac{2}{255}$	UNSAT%	46.5	49.0	48.5	42.0	50.0	51.0	47.5	44.0	24.0	9.0	12.0	39.0
	Stable%	79.3	76.2	80.4	91.6	77.6	69.6	74.8	94.2	53.4	42.3	44.1	80.3
	Time (s)	13.8	14.8	11.1	9.8	17.1	21.2	24.7	14.2	77.7	112.9	105.2	46.8
	Time _{U+T} (s)	16.2	18.0	11.1	7.7	20.6	27.5	33.9	15.8	114.9	158.1	150.9	68.3
	PGD ₁₀₀	51.3	53.8	49.9	50.9	53.5	59.3	55.1	48.2	62.7	64.5	65.3	57.8
$\frac{4}{255}$	UNSAT%	22.5	17.0	30.0	31.0	17.5	8.0	14.5	28.0	1.0	0.5	1.0	2.5
	Stable%	48.9	40.0	50.7	80.5	40.4	24.1	33.6	84.9	7.3	2.8	3.3	50.8
	Time (s)	39.3	56.3	33.1	17.9	61.5	80.4	61.4	27.3	101.8	104.3	104.7	90.4
	Time _{U+T} (s)	85.6	118.8	65.0	29.3	121.5	156.5	127.6	51.6	176.9	178.7	177.0	172.1
	PGD ₁₀₀	43.6	44.5	44.0	41.8	46.6	48.5	48.3	41.5	54.8	52.8	55.6	50.8
$\frac{6}{255}$	UNSAT%	5.0	2.5	9.0	17.0	1.0	1.0	1.5	12.5	1.0	0.0	0.0	1.0
	Stable%	23.4	15.9	24.3	68.0	14.0	5.7	9.7	73.7	1.1	0.4	0.4	44.3
	Time (s)	49.0	56.5	54.9	33.4	69.3	62.6	61.7	39.9	89.6	85.4	82.4	78.6
	Time _{U+T} (s)	153.2	167.9	140.8	87.8	175.2	175.0	172.6	112.3	176.3	180.0	180.0	178.6
	PGD ₁₀₀	36.8	35.5	38.5	33.0	39.5	37.9	41.1	36.0	47.4	40.9	45.4	44.4
$\frac{8}{255}$	UNSAT%	1.0	0.5	1.0	7.5	0.5	0.5	0.5	2.5	0.0	0.0	0.0	0.5
	Stable%	10.1	5.8	10.8	57.7	4.2	1.2	2.5	65.3	0.2	0.1	0.0	43.3
	Time (s)	45.8	44.0	54.3	34.3	54.4	43.4	53.3	44.9	75.0	62.7	65.2	66.5
	Time _{U+T} (s)	172.7	176.0	174.3	124.3	176.8	179.6	176.6	163.4	180.0	180.0	180.0	177.8
	PGD ₁₀₀	29.9	27.4	32.9	25.3	32.7	28.3	33.9	30.2	39.8	30.5	35.3	38.0

Table 5: Networks trained with $\varepsilon = 8/255$ on CIFAR-10 dataset with default parameters. The best results are highlighted in bold. Verified under $\varepsilon \in \{2/255, 4/255, 6/255, 8/255\}$. T: TRADES, M: Madry, R: ReLU stable, O: Our method.

Model		M1			M2			M3		
Method		T*	M*	R*	T*	M*	R*	T*	M*	R*
Test Acc.		-7.7%	-8.8%	-2.9%	-3.6%	-10.0%	-3.7%	-5.7%	-13.0%	-7.5%
$\varepsilon=0.1$	UNSAT%	+1.9	+6.0	-8.3	-2.6	+28.0	-6.4	+19.5	+48.5	+37.6
	Stable%	+52.7	+17.2	+14.8	+53.2	+28.9	+21.4	+71.6	+73.9	+82.6
	Time (s)	-17.6	-5.0	-3.6	-14.4	+8.5	-4.2	-32.7	-5.2	-57.1
	Time _{U+T} (s)	-25.1	-10.0	-4.3	-18.7	-52.7	-6.1	-34.6	-82.3	-72.7
	PGD ₁₀₀	-11.1	+7.6	-9.5	-11.4	+27.6	-7.9	-9.6	+36.5	-10.7
$\varepsilon=0.2$	UNSAT%	+11.9	-4.5	-7.7	-3.4	+0.5	-2.7	+0.1	+0.5	+49.1
	Stable%	+62.1	+29.5	+28.8	+54.0	+42.7	+38.5	+47.2	+45.8	+76.4
	Time (s)	-34.5	-19.1	-8.0	-20.7	+14.4	-9.9	-11.4	+37.6	-66.6
	Time _{U+T} (s)	-55.6	+7.3	-11.4	-1.8	-2.4	-15.9	-0.1	-0.6	-101.1
	PGD ₁₀₀	-16.8	-8.1	-14.7	-21.1	+2.7	-12.0	-11.0	+29.6	-13.8
$\varepsilon=0.3$	UNSAT%	+11.7	-0.4	-2.4	-0.1	0.0	+5.5	0.0	0.0	+30.6
	Stable%	+58.0	+40.0	+36.5	+49.0	+48.6	+47.8	+17.8	+2.1	+63.6
	Time (s)	-30.2	-25.6	-17.4	-29.7	-1.6	-22.5	-11.2	-16.5	-43.8
	Time _{U+T} (s)	-50.5	+1.5	-27.1	-0.3	0.0	-42.2	0.0	-120.0	-80.8
	PGD ₁₀₀	-19.5	-32.4	-19.5	-31.5	-26.6	-15.6	-14.5	+13.8	-17.2

Table 6: Networks trained with each method combined with our method on the Fashion-MNIST dataset with $\varepsilon = 0.3$. Improved results are highlighted in bold. T*: TRADES+Ours, M*: Madry+Ours, R*: ReLU Stable+Ours.

accuracy as adversarial perturbations increase, affirming its ability to maintain verification-friendly properties. Our approach consistently maintains a high ratio of stable neurons, even under the most challenging perturbation radii. This is particularly evident in the C2 and C3 models, where our method achieves a stable neuron ratio of over 50% at the highest perturbation radius. In contrast, other methods almost lose all stable neurons at the same perturbation radius.

Extra Results for RQ2

Table 6 and Table 7 show the results of networks trained with each method combined with our method on the Fashion-MNIST and CIFAR-10 datasets, respectively.

Our method significantly increases the ratio of stable neurons, which implies a smaller theoretical upper bound for solving. In most cases, the verification time is greatly reduced after combining our method. The UNSAT% slightly decreases when combined with our method at the smallest ε , but as the robustness radius ε increases, our method performs almost the best in terms of UNSAT%. It is worth not-

Model		C1			C2			C3		
Method		T*	M*	R*	T*	M*	R*	T*	M*	R*
Test Acc.		-9.2%	-14.2%	-8.1%	+5.4%	-11.0%	-0.1%	-0.2%	-9.3%	-13.4%
$\varepsilon = \frac{2}{255}$	UNSAT%	-6.0	-7.5	-7.5	-9.5	-4.0	-2.5	-0.9	+35.5	+32.5
	Stable%	+17.2	+17.8	+13.5	+14.3	+22.2	+17.2	+9.5	+45.7	+47.3
	Time (s)	-3.9	-6.3	-3.5	+8.2	-6.7	-11.0	+3.5	-85.4	-84.1
	Time _{U+T} (s)	-6.2	-11.5	-6.8	+19.4	-9.3	-17.1	+4.7	-120.0	-123.1
	PGD ₁₀₀	-7.9	-10.3	-6.5	-1.5	-7.8	-6.3	-0.5	-4.8	-18.6
$\varepsilon = \frac{4}{255}$	UNSAT%	+7.5	+15.0	+5.7	-10.5	+17.5	+2.5	+0.0	+2.5	+5.0
	Stable%	+42.7	+45.7	+35.3	+36.6	+52.4	+46.5	+15.2	+58.1	+76.1
	Time (s)	-23.3	-38.5	-20.6	-14.1	-44.9	-31.6	+1.0	-18.0	-46.5
	Time _{U+T} (s)	-58.6	-87.7	-48.5	+20.4	-82.9	-48.9	+3.1	-6.4	-25.5
	PGD ₁₀₀	-6.6	-5.9	-5.1	-9.2	-3.9	-12.0	-0.5	+0.3	-13.9
$\varepsilon = \frac{6}{255}$	UNSAT%	+13.5	+21.0	+15.5	0.0	+3.5	+0.5	-1.0	+0.5	+10.6
	Stable%	+62.2	+59.6	+53.0	+47.7	+50.1	+56.0	+16.5	+51.6	+77.3
	Time (s)	-22.8	-36.2	-35.4	-38.4	-5.2	-27.3	-2.0	-9.1	-33.0
	Time _{U+T} (s)	-85.2	-121.5	-99.7	-7.8	-15.4	-9.6	+3.7	0.0	-48.3
	PGD ₁₀₀	-5.4	-1.5	-4.2	-14.7	-0.4	-15.9	-0.6	+4.9	-8.8
$\varepsilon = \frac{8}{255}$	UNSAT%	+9.5	+10.1	+13.0	-0.5	+0.5	-0.5	0.0	0.0	+2.0
	Stable%	+67.9	+57.6	+56.7	+50.8	+39.1	+52.2	+16.1	+34.0	+69.2
	Time (s)	-16.6	-7.2	-22.4	-33.3	+0.9	-31.3	-7.5	+3.5	-13.9
	Time _{U+T} (s)	-69.5	-53.5	-81.8	+3.2	-7.0	+3.4	0.0	0.0	-12.2
	PGD ₁₀₀	-3.6	+2.0	-2.7	-17.7	+2.2	-17.8	-0.1	+7.9	-3.2

Table 7: Networks trained with each method combined with our method on the CIFAR-10 dataset with $\varepsilon = 8/255$. Improved results are highlighted in bold. T*: TRADES+Ours, M*: Madry+Ours, R*: ReLU Stable+Ours.

Model	Method	Test Acc	UNSAT%	#UNSAT	Time	Time _{U+T}	PGD ₅₀	PGD ₁₀₀	Stable%
C1	TRADES	69.8	38.5	77	43.4	67.3	55.8	55.8	53.0
	Madry	69.6	39.5	79	41.7	63.8	54.3	54.3	50.8
	RS	69.3	44.5	89	30.9	44.4	56.7	56.7	60.9
	Ours	69.0	46.0	92	27.3	37.8	56.4	56.4	77.6
	RS	75.0	1.5	3	49.9	171.9	26.4	26.4	8.5
	Ours	75.0	33.0	66	54.4	87.0	56.1	56.1	46.3
C2	Natural	77.6	0.5	1	49.6	178.4	10.0	10.0	5.3
	TRADES	74.7	35.0	70	55.0	85.3	60.4	60.4	46.9
	Madry	74.4	28.5	57	65.5	103.1	58.7	58.8	39.4
	RS	74.4	41.5	83	53.9	77.1	61.4	61.4	49.4
	Ours	74.0	45.5	91	38.8	55.0	61.3	61.3	56.8
	RS	79.3	1.0	2	54.1	173.9	28.5	28.4	3.7
C3	Ours	79.3	12.0	24	87.9	147.3	57.3	57.2	26.3
	Natural	80.6	0.5	1	53.3	181.0	10.0	10.0	2.8
	TRADES	77.6	5.5	11	112.8	165.9	64.0	64.0	27.7
	Madry	77.8	1.0	2	113.9	177.2	60.1	60.1	17.0
	RS	78.0	2.5	5	122.2	176.8	61.1	61.2	21.9
	Ours	77.0	25.6	51	95.4	126.2	66.7	66.7	80.1
	RS	83.7	0.0	0	65.5	180.4	30.3	30.3	0.1
	Ours	83.3	1.0	2	115.6	177.3	61.0	61.0	5.6
	Natural	84.2	0.0	0	68.0	184.1	10.0	10.0	0.0

Table 8: Networks trained on CIFAR-10 dataset with $\varepsilon = 2/255$. The best results are highlighted in bold. 'Natural' denotes the accuracy when only CE loss is used.

ing that, in the largest model, combining our method almost improves all metrics, and the decrease in test accuracy and PGD accuracy is not significant. Especially in the Fashion-MNIST dataset, after combining our method, the UNSAT% of the RS method in M3, $\varepsilon = 0.3$ increases from 0.0 to 30%, which is a significant improvement considering the verification capability of the solver.

When combining our method with other training meth-

ods, the network's verification performance is significantly improved; however, the test accuracy and robustness may be reduced. It needs a trade-off between verification performance and robustness depending on the application scenario when combining our method with other training methods.

Model	ε	$\gamma[i]$	Test Acc	UNSAT%	Time	Time _{U+T}	PGD ₁₀₀	Stable%
M1	0.1	1	97.61	100	3.24	3.24	51.16	89.8
		$2^{r[i]}$	98.61	100	3.22	3.22	52.18	85.9
		$r[i] \cdot m[i]$	98.88	98	3.05	3.12	53.66	75.3
C1	$\frac{2}{255}$	1	68.10	36	23.56	42.40	95.46	66.55
		$2^{r[i]}$	69.53	35	35.83	63.57	97.46	62.05
		$r[i] \cdot m[i]$	71.15	32	44.53	77.45	97.83	51.37

Table 9: Networks trained with different $\gamma[i]$ on CIFAR-10 dataset and MNIST dataset.

Model	ε	Method	Test Acc	UNSAT%	Time	Time _{U+T}	PGD ₁₀₀	Stable%
M1	0.1	SABR	89.25	22	26.89	20.74	25.91	84.16
		NBC	97.61	100	3.22	3.22	97.47	89.78
C1	$\frac{2}{255}$	SABR	59.57	50	6.55	3.49	48.53	87.57
		NBC	62.48	54	6.69	5.02	51.55	79.60

Table 10: Comparison of networks trained with NBC and SABR on CIFAR-10 dataset and MNIST dataset.

β	0.0	1.0	3.0	6.0	9.0
Test Acc	76.0	72.2	70.0	67.1	66.0
UNSAT%	0	22.0	34.0	32.0	32.0
Stable%	4.8	42.1	60.9	71.8	74.3
Time (s)	44.4	45.4	39.9	23.7	19.4
Time _{U+T} (s)	180	96.1	71.0	42.9	34.4
PGD ₁₀₀	0.8	49.1	53.2	52.5	52.5

Table 11: Networks (C1 model) trained with NBC at $\varepsilon = 2/255$ on CIFAR-10 dataset with different β .

Discussion for Hyperparameters

Table 11 shows the results of C1 networks trained with NBC at $\varepsilon = 2/255$ on CIFAR-10 dataset with different β . We evaluated the models with 50 verification tasks. Overall, as β increases, the test accuracy decreases, UNSAT% increases, stable neuron ratio increases, verification time decreases, which is consistent with our expectations. The results show that a larger β can improve the verification performance of the network, but it may reduce the accuracy of the network. Therefore, it is necessary to choose an appropriate β according to the specific requirements of the application scenario.

Table 9 shows the results of networks trained with different $\gamma[i]$ on CIFAR-10 dataset and MNIST dataset. We evaluated the models with 50 verification tasks. As discussed in the main paper, neurons in smaller layers, when behavior is consistent, may constrain subsequent layers through propagation. Moreover, layers near the input and output often have fewer neurons, applying constraints to these layers can directly affect the forward or backward propagation process and accelerate the convergence of target loss. In contrast, middle layers typically have more neurons and are responsible for extracting complex features; over-constraining these layers could adversely affect the model’s expressive power. The results show that using a looser penalty on layers with more neurons may slightly decrease accuracy but increase the proportion of stable neurons and improve verification

speed, which is consistent with our expectations.

Compare with Certified Training

Table 10 shows the comparison of networks trained with NBC and SABR. We evaluated the models with 50 verification tasks. In the MNIST dataset, the network trained with NBC achieves better performance in all metrics compared to the network trained with SABR. In the CIFAR-10 dataset, the network trained with NBC achieves better performance in terms of Test accuracy, UNSAT% and the accuracy under the PGD attack. These results show that under the same network architecture, our method—despite its lower computational cost and ease of implementation—achieves performance comparable to, or even surpasses, that of certified training methods which demand more computational resources.